



OPEN ACCESS

EDITED BY

Nick Varley,
University of Colima, Mexico

REVIEWED BY

Luis E. Lara,
Austral University of Chile, Chile
Nicholas Barber,
Washington and Lee University, United States
Rebecca Williams,
University of Hull, United Kingdom

*CORRESPONDENCE

Dini Nurfiani,
✉ dnurfianeart@gmail.com

RECEIVED 23 June 2023

ACCEPTED 22 January 2024

PUBLISHED 15 February 2024

CITATION

Nurfiani D, Ismail T, Pratama A, Rukmini NA, Abdurrachman M, Kurniawan IA, Draniswari WA, Banggur WFS and Suryanata PB (2024), Geochemical characteristics of Anak Krakatau's (Indonesia) lava in the past half-century. *Front. Earth Sci.* 12:1245001. doi: 10.3389/feart.2024.1245001

COPYRIGHT

© 2024 Nurfiani, Ismail, Pratama, Rukmini, Abdurrachman, Kurniawan, Draniswari, Banggur and Suryanata. This is an open-access article distributed under the terms of the [Creative Commons Attribution License \(CC BY\)](https://creativecommons.org/licenses/by/4.0/). The use, distribution or reproduction in other forums is permitted, provided the original author(s) and the copyright owner(s) are credited and that the original publication in this journal is cited, in accordance with accepted academic practice. No use, distribution or reproduction is permitted which does not comply with these terms.

Geochemical characteristics of Anak Krakatau's (Indonesia) lava in the past half-century

Dini Nurfiani^{1*}, Taufik Ismail^{1,2,3}, Aditya Pratama^{1,2}, Niken Angga Rukmini⁴, Mirzam Abdurrachman^{2,3}, Idham Andri Kurniawan^{2,3}, Windi Anarta Draniswari¹, Wilfridus Ferdinando Supriyadi Banggur^{1,2} and Putu Billy Suryanata^{1,5}

¹Research Center for Geological Disaster, National Research and Innovation Agency, Bandung, Indonesia, ²Faculty of Earth Sciences and Technology, Bandung Institute of Technology, Bandung, Indonesia, ³Department of Geology, Indonesia College of Mineral Technology, Bandung, Indonesia, ⁴Balai Penyelidikan dan Pengembangan Teknologi dan Kebencanaan Geologi, Center for Volcanology and Geological Hazard Mitigation, Geological Agency of Indonesia, Yogyakarta, Indonesia, ⁵Faculty of Mining and Petroleum Engineering, Bandung Institute of Technology, Bandung, Indonesia

KEYWORDS

Anak Krakatau, basaltic lava, petrology, geochemistry, crystal size distribution (CSD)

1 Introduction

Anak Krakatau Volcano is located in the Sunda Strait, between Sumatra and Java islands, and surrounded by three islands (i.e., Panjang, Rakata, and Sertung), which are the remnants of ancient Krakatau. After the last caldera-forming eruption in 1883, the activity of the volcano resumed in 1927 with Surtseyan eruptions (Camus et al., 1987; Schipper and White, 2016), which later formed Anak Krakatau (AK). Since then, AK has erupted frequently, every 1 to 3 years, with a Volcanic Explosivity Index (VEI) of 1–2, except for the 2018 eruption, whose VEI of 3 (Global Volcanism Program, 2023) led to the flank collapse event that caused tsunamis. Since that event, the volcano has produced episodic eruptions until the present (end of 2023) (Global Volcanism Program, 2023).

Previous petrological and geochemical studies at AK predominantly involved products from the early eruptive history of AK (see [Supplementary Table S1](#)). The post-1996 products consisting of lava flow, ballistic blocks, and scoria from pyroclastic deposits are basaltic andesite in composition (Ardian et al., 2022). A few studies have been reported on the chemical compositions of recent eruptive materials. Fiantis et al. (2021) analyzed the 2018 volcanic deposits, i.e., ash and lapilli, resulting in two group compositions with a low SiO₂ content (mean 39.01 wt%) and basaltic andesite (mean 54.93 wt%). Cutler et al. (2022) also reported the groundmass glass compositions of 2018 ash samples, which are andesitic. The latest lava product analyzed was from the 2020 eruption and has a basaltic composition, as reported by Pratama et al. (2023). They also analyzed older products of Krakatau even prior to the 1883 caldera-forming eruption, which were more evolved in composition, i.e., andesitic to rhyolitic.

Meanwhile, it can be proposed that the Anak Krakatau plumbing system consists of multiple magma storage regions, with depths ranging from intermediate to up to 26 km (Dahren et al., 2012; Agangi and Reddy, 2016; Pratama et al., 2023). Gardner et al. (2012) also revealed a complex plumbing system consisting of many small but shallow magma pockets beneath Anak Krakatau. Madden-Nadeau et al. (2021) suggested that different melt-rich regions in the shallow system coalesced and mixed over certain periods, leading to the 1883 climactic eruption. Continuous integrated multi-discipline studies are crucial to

monitoring the evolution of the Anak Krakatau volcanic activity. Recent visual, seismicity, and deformation data analyses infer the potential hazards from the current activity with lava flows, ballistics, and volcanic ash resulting from Vulcanian and/or Strombolian eruptions (Kristianto et al., 2021).

Not many of these studies measured the matrix–glass compositions, which are commonly used for inferring magma differentiation and/or the evolution of magma compositions through time, combined with both (1) whole-rock and (2) mineral (titanomagnetite) compositions (de Maisonneuve et al., 2021; Keller et al., 2023). Our study provides a compilation of petrological and geochemical data on the lava products of 1973–2017, including the major element compositions of whole-rock, matrix-glass, and minerals. The aim of this study is to investigate the temporal evolution of magma composition at Anak Krakatau. We first performed petrography analysis to determine mineral assemblages and their proportions. The analysis of the chemistry and proportion of minerals in samples produced from different eruptions would infer whether or not there are any changes in the magma storage conditions. The matrix–glass compositions are also used to track magma differentiation in the past half-century. In addition, we applied crystal size distribution (CSD) (Cashman and Marsh, 1988) to obtain the (plagioclase) crystal residence times. The crystals formed in magma storage reflect the crystal growth rate and duration the magma remained stalled at a certain depth (Marsh, 1988; Higgins, 2000; Morgan and Jerram, 2006). Therefore, the plagioclase crystal residence time could indicate magma residence times in the reservoir.

This study provides valuable data as sampling older lava products can no longer be done since they have vanished along with the collapse of the west sector of the Krakatau volcanic edifice during the 2018 eruption (Grilli et al., 2019; Williams et al., 2019; Omira and Ramalho, 2020; Perttu et al., 2020; Zengaffinen et al., 2020). According to Pratama et al. (2023), AK is currently in the incubation phase in terms of a caldera cycle concept. De Maisonneuve et al. (2021) defined the incubation or “preheating” phase as the thermal maturation of the crust when mafic magmas migrate through the pre-existing crust. The characteristics of this phase are indicated by mafic products from frequent and small eruptions (VEI 1–2), as shown by the recent Anak Krakatau activity. Therefore, this study could offer basic information regarding the AK eruptive products over time, which can contribute to monitoring the possible temporal changes in a caldera cycle.

2 Samples

We used 13 lava samples obtained from the volcano–stratigraphy study of Ismail et al. (2020), where the sampling location sites are shown in Supplementary Figure S1. All the samples of Ismail et al. (2020), which are mostly from Anak Krakatau eruptive products, were stored in a workshop room at the Department of Geology, Indonesia, College of Mineral Technology. Following up on the volcano–stratigraphy study, we recently analyzed all the Anak Krakatau lava samples spanning from 1973 until 2017. The lava flow deposits are characterized as auto-breccia and aa lava, where the latter dominates the most. In general, the samples have a porphyritic texture and are mostly grayish in color, except for a

few samples showing a reddish color, i.e., the 2014/ST73 product (Supplementary Figure S2). Hand sample observations show that the lava products of 1981, 1992, 1997, 1999, 2007, 2012, and 2017 are crystal-rich, while the rest have a relatively low crystal content.

3 Methods

The loss on ignition (LOI) measurement was done on dry powder samples using a Carbolite HTF High-Temperature Chamber Furnace (Carbolite Gero, United Kingdom) at the Advanced Characterization Laboratory, National Research and Innovation Agency of Republic Indonesia (Badan Riset dan Inovasi Nasional—BRIN). The LOI measurements were carried out twice on each sample and averaged. Approximately 1 g of the sample was heated to 105°C–110°C and then placed in a porcelain bowl whose weight was already known. It was heated to 400°C for 30 min before the temperature was increased to 1,000°C and left for 20 min. Afterward, the sample was cooled in a desiccator vacuum for 20 min and then weighed.

The whole-rock compositions of all samples were measured on pressed pellets using a Bruker S2 Puma XY X-Ray Fluorescence (XRF) spectrometer with a power of 50 W, a current of 2 mA, and an accelerating voltage of 50 kV at the Advanced Characterization Laboratories Serpong, National Research and Innovation Agency (Badan Riset dan Inovasi Nasional, BRIN). The spectrometer was calibrated using the FluXana FLX-K04/BAXS-S2 glass disc that was also used for drift monitoring. All samples were thin-sectioned for further analyses. The thin sections (0.03-mm-thick) were examined under an optical microscope to determine mineral assemblages and abundances. We determined the mineral percentage through visual semi-quantitative estimation, relying on a mineralogical chart for reference. Observations were conducted on five sections of the thin section, specifically in the upper right, upper left, middle, lower right, and lower left regions. Each section included a circular region with a diameter of 2 mm. The mineral percentage values for each section were then averaged to obtain modal mineral composition data that represented the respective thin section. This visual approach aids us in quickly estimating mineral percentages. The potential for errors exists, predominantly in the form of overestimating small percentages. To mitigate such errors, we employ the visual chart proposed by Reid (1985) for percentages below 1% and refer to the methodology outlined by Terry and Chilingar (1955) for percentages exceeding 1%.

The surface of thin sections was polished using a series of successive diamond pastes (6, 3, 1, and ¼ µm) and then examined using a scanning electron microscope (FEI Quanta 650 FEG) equipped with an energy dispersive X-ray spectroscopy (EDS) detector at Badan Penyelidikan dan Pengembangan Teknologi Kebencanaan Geologi (BPPTKG Yogyakarta)—Center for Volcanology and Geological Hazard Mitigation (CVGHM) to measure the compositions of minerals, matrix–glass, and/or melt inclusions. The backscattered electron images were taken with an accelerating voltage range of 10–20 kV and a spot size varying between 4 and 5. Meanwhile, EDS data were acquired using the point analysis method and measured for 5 s. Data acquisition uses AZtec (Oxford Instruments NanoAnalysis-OINA MicroAnalysis System), and the data were qualitatively calibrated. The results of

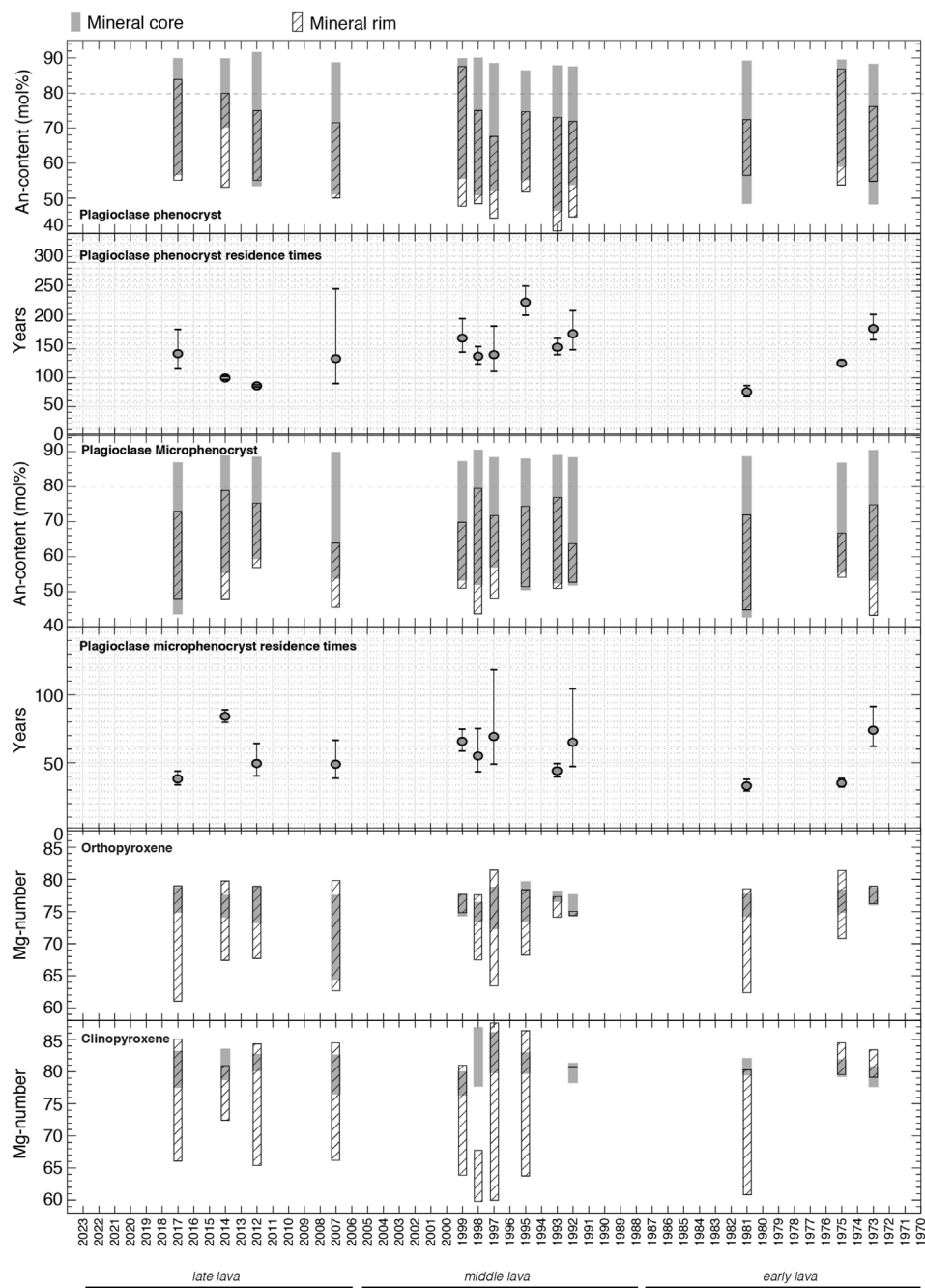


FIGURE 2
Temporal evolution of the An content of plagioclase and Mg number of pyroxene, as well as the estimates of residence times.

Although the whole-rock compositions are basaltic, their matrix–glass compositions are more evolved, and most of them are dacitic–rhyolitic (Figure 1A; Supplementary Table S3). Even the earlier 1973 lava has andesitic–dacitic matrix–glass compositions. Figure 1A shows that the matrix–glass compositions have a dominant SiO₂ content of ~60–70 wt%. However, the 1999 lava has the most evolved matrix–glass composition, reaching ~78 wt% of the SiO₂ content. Representative BSE images of matrix–glass are shown in Supplementary Figure S5. Meanwhile, the melt inclusions are generally present in orthopyroxene/clinopyroxene

and plagioclase hosts. However, the melt inclusions affected by post-entrapment processes (e.g., containing daughter minerals) are quite dominant (Supplementary Figure S6); hence, we do not report the melt inclusion composition data in Supplementary Table S1.

4.2 Mineralogy and mineral compositions

The crystal content in all samples varies from ~9 to 32% (Figure 1B), with the ST75 (1973) and ST79 (1981) samples having

the lowest and highest crystal content, respectively. Each sample contains plagioclase, orthopyroxene, clinopyroxene, olivine, and oxide minerals (magnetite). There is no significant difference in the occurrence of minerals in each sample. Representative thin section images are shown in [Supplementary Figure S7](#).

4.2.1 Plagioclase

Plagioclase makes up the most abundant mineral in each sample (~5–24%), which governs the proportion of the total crystal content ([Figure 1B](#)). The crystals are generally anhedral to euhedral and are 0.08–1.54 mm on average. Plagioclase minerals appear to have a low abundance in younger products (late lava). It can be seen in [Figure 1B](#) that the plagioclase content in middle and early lava is dominantly >10% (except 1973 and 1995 lavas), while the latest four samples (2007, 2012, 2014, and 2017 lava) contain approximately 10% plagioclase minerals.

The members of plagioclase in all samples are mostly andesine, labradorite, and bytownite ([Supplementary Figure S8](#)). Both micro- and phenocrysts of plagioclase have a wide range of compositions with An_{40-90} ([Figure 2](#)), where calcic plagioclase is dominant. For plagioclase phenocrysts, all samples contain a high An core ($>An_{80}$); however, the samples with a high An rim ($>An_{80}$) are the 1975, 1999, and 2017 lavas. For plagioclase microphenocrysts, a similar high An core is also observed in all samples, while no microphenocryst rims have a high An-content of $>An_{80}$, except for the 1998 and 2014 samples that are close to An-rim₈₀. The wide range of the An-content is reflected by various plagioclase textures found, such as sieve, skeletal, and normal zoning ([Supplementary Figure S9](#)).

4.2.2 Pyroxene

Pyroxene in all samples consists of clinopyroxene (augite and pigeonite) and orthopyroxene (enstatite) ([Supplementary Figure S8](#)), where their proportions at each sample do not exceed 5% ([Figure 1B](#)). Orthopyroxene has a size of 0.07–0.46 mm and has subhedral to euhedral shapes, while clinopyroxene has a size of 0.01–0.37 mm with subhedral to euhedral crystal shapes. The proportion of pyroxene does not significantly vary with time, particularly for clinopyroxene.

The core and rim compositions of orthopyroxene have Mg numbers within the 60–80 range, with the core having a narrower range of Mg numbers (Mg_{70-80}) than the rim ([Figure 2](#)). The Mg core of 2007 lava extends lower to Mg_{65} than that of other lavas. As an exception, the 1973, 1992, 1993, and 1999 lavas have both narrow ranges of Mg core and Mg rim. Meanwhile, most of the clinopyroxene (core and/or rim) contains an Mg number higher than that of orthopyroxene (i.e., $>Mg_{80}$). Similar to orthopyroxene, clinopyroxene is generally characterized by narrow ranges of Mg core (Mg_{76-87}) and wide ranges of Mg rim (Mg_{60-88}). The dominant texture found in pyroxene is unzoned ([Supplementary Figure S9](#)).

4.2.3 Olivine

Olivine only takes up approximately 1% of all samples and is present as microphenocrysts with sizes of 0.02–0.12 mm. We did not observe olivine in the 1973 and 1998 lavas. Their compositions are distributed into forsterite end-members ([Supplementary Figure S8](#)).

4.2.4 Oxide minerals

The proportion of oxide minerals does not exceed 3%, and they are generally present as microphenocrysts with a size of 0.04–0.13 mm on average. The oxide minerals exist both as individual crystals and within plagioclase or pyroxene crystals.

4.3 CSD

[Figure 2](#) also shows the magma residence time estimated from plagioclase micro- and phenocrysts. For the phenocrysts, the magmas producing all lava samples were stored for ~100–230 years, except for the samples from 1981 and 2012, which were stored for ~75 and 85 years, respectively. On average, they were typically stored for approximately 142 years. Meanwhile, the residence times of plagioclase microphenocrysts are between 33 and 84 years, with an average of ~55 years. The supporting data for the residence time calculation can be found in [Supplementary Table S1](#).

5 Conclusion

Overall, this dataset provides fundamental geochemical data and residence times of Anak Krakatau lavas prior to the 2018 collapse event. The petrography and geochemical analyses indicate the following:

- 1) The compositions of all AK lava products are predominantly basaltic, implying there are no changes toward more evolved magma compositions. However, the matrix–glass compositions of all samples indicate a more evolved, mostly dacitic–rhyolitic composition.
- 2) All samples dominantly consist of similar mineral assemblages of plagioclase, two-pyroxene, and oxide minerals, with fewer proportions of olivine. No hydrous minerals are observed.
- 3) All lavas contain plagioclase micro- and phenocrysts that have a high An core ($>An_{80}$). Meanwhile, plagioclase phenocrysts that contain both a high An core and rim ($>An_{80}$) were observed in the 1975, 1999, and 2017 lavas.
- 4) Both ortho- and clinopyroxene contain a narrower range of Mg-number core than the rim. In each pyroxene, some samples have a Mg-number rim slightly higher than the core.
- 5) On average, plagioclase phenocrysts and microphenocrysts were stored for approximately 142 years and 55 years, respectively.

Data availability statement

The original contributions presented in the study are included in the article/[Supplementary Material](#); further inquiries can be directed to the corresponding author.

Author contributions

DN and TI contributed as the main contributors of this paper. DN, AP, and NR performed SEM-EDS analysis. TI, WB, MA, and IK

collected the samples in the field. DN, TI, and WD analyzed CSD and geochemical data. DN and TI wrote the first draft of the manuscript. All authors contributed to the article and approved the submitted version.

Funding

This study was supported financially by the Earth Science and Maritime Research Organization, National Research and Innovation Agency of the Republic of Indonesia through Rumah Program Kebencanaan (No. SP DIPA-124.01.1.690501/2022 and SP DIPA -124.01.1.690501/2023) grant to DN, AP, and MA. Additional funding was also received from the Faculty of Earth Sciences and Technology, Institut Teknologi Bandung through Post-Doctoral Research Grants to AP (No. 1798/IT1.C01/SK-KP/2022 and 1607A/IT1.C01/SPK-KP.01/2023). This study was also supported by the Post-Doctoral Research Grant from the National Research and Innovation Agency Republic of Indonesia (BRIN) to DN (No. 64/II/HK/2022).

Acknowledgments

Permission to conduct field research at Krakatau volcano was given by the BKSDA (Balai Konservasi Sumber Daya Alam or Natural Resource Conservation Center) of Bengkulu Lampung,

References

- Abdurrachman, M., Widiyantoro, S., Priadi, B., and Ismail, T. (2018). Geochemistry and structure of Krakatau volcano in the Sunda Strait, Indonesia. *Geosciences* 8 (4), 111. doi:10.3390/geosciences8040111
- Angari, A., and Reddy, S. M. (2016). Open-system behaviour of magmatic fluid phase and transport of copper in arc magmas at Krakatau and Batur volcanoes, Indonesia. *J. Volcanol. Geotherm. Res.* 327, 669–686. doi:10.1016/j.jvolgeores.2016.10.006
- Ardian, D. N., Darmawan, H., Mutaqin, B. W., and Haerani, N. (2022). Grain size, mineralogical, and geochemistry of the 1996–2018 volcanic products of Anak Krakatau volcano, Indonesia. *IOP Conf. Ser. Earth Environ. Sci.* 1071 (1), 012017. doi:10.1088/1755-1315/1071/1/012017
- Bas, M. L., Maitre, R. L., Streckeisen, A., and Zanettin, B. (1986). A chemical classification of volcanic rocks based on the total alkali-silica diagram. *J. Petrology* 27 (3), 745–750. doi:10.1093/ptrology/27.3.745
- Camus, G., Gourgaud, A., and Vincent, P. M. (1987). Petrologic evolution of Krakatau (Indonesia): implications for a future activity. *J. Volcanol. Geotherm. Res.* 33 (4), 299–316. doi:10.1016/0377-0273(87)90020-5
- Cashman, K. V. (1993). Relationship between plagioclase crystallization and cooling rate in basaltic melts. *Contributions Mineralogy Petrology* 113, 126–142. doi:10.1007/BF00320836
- Cashman, K. V., and Marsh, B. D. (1988). Crystal size distribution (CSD) in rocks and the kinetics and dynamics of crystallization II: makaopuhi lava lake. *Contributions Mineralogy Petrology* 99 (3), 292–305. doi:10.1007/bf00375363
- Cutler, K. S., Watt, S. F., Cassidy, M., Madden-Nadeau, A. L., Engwell, S. L., Abdurrachman, M., et al. (2022). Downward-propagating eruption following vent unloading implies no direct magmatic trigger for the 2018 lateral collapse of Anak Krakatau. *Earth Planet. Sci. Lett.* 578, 117332. doi:10.1016/j.epsl.2021.117332
- Dahren, B., Troll, V. R., Andersson, U. B., Chadwick, J. P., Gardner, M. F., Jaxybulatov, K., et al. (2012). Magma plumbing beneath Anak Krakatau volcano, Indonesia: evidence for multiple magma storage regions. *Contributions Mineralogy Petrology* 163, 631–651. doi:10.1007/s00410-011-0690-8
- de Maisonville, C. B., Forni, F., and Bachmann, O. (2021). Magma reservoir evolution during the build up to and recovery from caldera-forming eruptions—A generalizable model? *Earth-Science Rev.* 218, 103684. doi:10.1016/j.earscirev.2021.103684
- Indonesia. The authors thank Muhammad Zain Tuakia, Cinantya Nirmala Dewi, and Mohammad Hasib for the fruitful discussion and their assistance with the laboratory work.
- Fiantis, D., Ginting, F. I., Gusnidar, M., Van Ranst, E., and Minasny, B. (2021). Geochemical characterization and evolution of soils from Krakatau Islands. *Eurasian Soil Sci.* 54, 1629–1643. doi:10.1134/s1064229321110077
- Gardner, M. F., Troll, V. R., Gamble, J. A., Gertisser, R., Hart, G. L., Ellam, R. M., et al. (2012). Crustal differentiation processes at Krakatau volcano, Indonesia. *J. Petrology* 54 (1), 149–182. doi:10.1093/ptrology/egs066
- Global Volcanism Program (2023). Volcanoes of the world (v. 5.1.4; 9 nov 2023). https://volcano.si.edu/gvp_votw.cfm.
- Grilli, S. T., Tappin, D. R., Carey, S., Watt, S. F., Ward, S. N., Grilli, A. R., et al. (2019). Modelling of the tsunami from the december 22, 2018 lateral collapse of Anak Krakatau volcano in the Sunda straits, Indonesia. *Sci. Rep.* 9 (1), 11946. doi:10.1038/s41598-019-48327-6
- Higgins, M. D. (2000). Measurement of crystal size distributions. *Am. Mineralogist* 85 (9), 1105–1116. doi:10.2138/am-2000-8-901
- Innocenti, S., Del Marmol, M.-A., Voight, B., Andreastuti, S., and Furman, T. (2013). Textural and mineral chemistry constraints on evolution of Merapi Volcano, Indonesia. *J. Volcanol. Geotherm. Res.* 261, 20–37. doi:10.1016/j.jvolgeores.2013.01.006
- Keller, F., Guillong, M., Geshi, N., Miyakawa, A., and Bachmann, O. (2023). Tracking caldera cycles in the Aso magmatic system—Applications of magnetite composition as a proxy for differentiation. *J. Volcanol. Geotherm. Res.* 436, 107789. doi:10.1016/j.jvolgeores.2023.107789
- Klein, J., Mueller, S. P., and Castro, J. M. (2017). The influence of crystal size distributions on the rheology of magmas: new insights from analog experiments. *Geochem. Geophys. Geosystems* 18 (11), 4055–4073. doi:10.1002/2017gc007114
- Kristianto, Indrastuti, N., Basuki, A., Purnamasari, H. D., Adi, S., Patria, C., et al. (2021). Potential eruption and current activity of Anak Krakatau volcano, Indonesia. *IOP Conf. Ser. Earth Environ. Sci.* 873 (1), 012021. doi:10.1088/1755-1315/873/1/012021
- Madden-Nadeau, A. L., Cassidy, M., Pyle, D. M., Mather, T. A., Watt, S. F. L., Engwell, S. L., et al. (2021). The magmatic and eruptive evolution of the 1883 caldera-forming eruption of Krakatau: integrating field-to crystal-scale observations. *J. Volcanol. Geotherm. Res.* 411, 107176. doi:10.1016/j.jvolgeores.2021.107176
- Marsh, B. D. (1988). Crystal size distribution (CSD) in rocks and the kinetics and dynamics of crystallization: I. Theory. *Contributions Mineralogy Petrology* 99, 277–291. doi:10.1007/bf00375362

Conflict of interest

The authors declare that the research was conducted in the absence of any commercial or financial relationships that could be construed as a potential conflict of interest.

Publisher's note

All claims expressed in this article are solely those of the authors and do not necessarily represent those of their affiliated organizations, or those of the publisher, the editors, and the reviewers. Any product that may be evaluated in this article, or claim that may be made by its manufacturer, is not guaranteed or endorsed by the publisher.

Supplementary material

The Supplementary Material for this article can be found online at: <https://www.frontiersin.org/articles/10.3389/feart.2024.1245001/full#supplementary-material>

- Mock, A., and Jerram, D. A. (2005). Crystal size distributions (CSD) in three dimensions: insights from the 3D reconstruction of a highly porphyritic rhyolite. *J. Petrology* 46 (8), 1525–1541. doi:10.1093/petrology/egi024
- Morgan, D. J., and Jerram, D. A. (2006). On estimating crystal shape for crystal size distribution analysis. *J. Volcanol. Geotherm. Res.* 154 (1–2), 1–7. doi:10.1016/j.jvolgeores.2005.09.016
- Nugroho, R. P., Disando, T., Kurniawan, I. A., and Abdurrachman, M. (2019). Crystal size distribution (CSD) of plagioclase phenocryst-microphenocryst and the calculation of crystal resident times in the continuous central eruption sequences of Mount Lasem, Central Java, Indonesia. *J. Phys. Conf. Ser.* 1363, 012041. doi:10.1088/1742-6596/1363/1/012041
- Oba, N., Tomita, K., Yamamoto, M., Istidjab, M., Badruddin, M., and Parlin, M. (1982). Geochemical study of lava flows, ejecta and pyroclastic flow from the Krakatau Group, Indonesia. *Kagoshima. Daigaku Rigakubu Kiyō. Chigaku seibutsugaku* (15), 41–76.
- Omira, R., and Ramalho, I. (2020). Evidence-calibrated numerical model of December 22, 2018, Anak Krakatau flank collapse and tsunami. *Pure Appl. Geophys.* 177, 3059–3071. doi:10.1007/s00024-020-02532-x
- Perttu, A., Caudron, C., Assink, J. D., Metz, D., Tailpied, D., Perttu, B., et al. (2020). Reconstruction of the 2018 tsunamigenic flank collapse and eruptive activity at Anak Krakatau based on eyewitness reports, seismo-acoustic and satellite observations. *Earth Planet. Sci. Lett.* 541, 116268. doi:10.1016/j.epsl.2020.116268
- Pratama, A., Nurfiani, D., Suryanata, P. B., Ismail, T., Bunga Naen, G. N. R., Abdurrachman, M., et al. (2023). Magma storage conditions beneath Krakatau, Indonesia: insight from geochemistry and rock magnetism studies. *Front. Earth Sci.* 11, 1128798. doi:10.3389/feart.2023.1128798
- Rasband, W. (1997). *ImageJ*, Bethesda, Maryland, USA: National Institute of Mental Health.
- Schipper, C. I., and White, J. D. (2016). Magma-slurry interaction in Surtseyan eruptions. *Geology* 44 (3), 195–198. doi:10.1130/g37480.1
- Terry, R. D., and Chilingar, G. V. (1955). Summary of "Concerning some additional aids in studying sedimentary formations," by MS Shvetsov. *J. Sediment. Res.* 25 (3), 229–234. doi:10.1306/74d70466-2b21-11d7-8648000102c1865d
- Westerveld, J. (1952). Quaternary volcanism on Sumatra. *Geol. Soc. Am. Bull.* 63 (6), 561–594. doi:10.1130/0016-7606(1952)63[561:qvovs]2.0.co;2
- Williams, R., Rowley, P., and Garthwaite, M. C. (2019). Reconstructing the Anak Krakatau flank collapse that caused the December 2018 Indonesian tsunami. *Geology* 47 (10), 973–976. doi:10.1130/g46517.1
- Zen, M. T., and Hadikusumo, D. (1964). Recent changes in the Anak-Krakatau volcano. *Bull. Volcanol.* 27, 259–268. doi:10.1007/bf02597525
- Zengaffinen, T., Løvholt, F., Pedersen, G. K., and Muhari, A. (2020). Modelling 2018 Anak Krakatau Flank Collapse and Tsunami: effect of landslide failure mechanism and dynamics on tsunami generation. *Pure Appl. Geophys.* 177, 2493–2516. doi:10.1007/s00024-020-02489-x